TM 851130

NAVAL UNDERWATER SYSTEMS CENTER
NEW LONDON LABORATORY
NEW LONDON, CONNECTICUT 06320

Technical Memorandum

LOW FREQUENCY ATTENUATION IN THE ARCTIC OCEAN (U)

Date: 1 September 1985 Prepared by:

F. R. DiNapoli
Arctic Warfare Office
Naval Underwater Systems Center
New London, CT. 06320

R. H. Mellen
Planning Systems Inc.
Marine Sciences
New London, CT. 06320

Report Documentation Page

Form Approved
OMB No. 0704-0188

1. REPORT DATE	2. REPORT TYPE	3. DATES COVERED
01 SEP 1985	**Technical Memo**	**01-09-1985 to 01-09-1985**

4. TITLE AND SUBTITLE
Low Frequency Attenuation in the Arctic Ocean

5a. CONTRACT NUMBER

5b. GRANT NUMBER

5c. PROGRAM ELEMENT NUMBER

6. AUTHOR(S)
F. DiNapoli; R. Mellen

5d. PROJECT NUMBER
C64666

5e. TASK NUMBER
14A

5f. WORK UNIT NUMBER

7. PERFORMING ORGANIZATION NAME(S) AND ADDRESS(ES)
Naval Underwater Systems Center,New London,CT,06320

8. PERFORMING ORGANIZATION REPORT NUMBER
TM 851130

9. SPONSORING/MONITORING AGENCY NAME(S) AND ADDRESS(ES)
Office of Naval Research

10. SPONSOR/MONITOR'S ACRONYM(S)

11. SPONSOR/MONITOR'S REPORT NUMBER(S)

12. DISTRIBUTION/AVAILABILITY STATEMENT
Approved for public release; distribution unlimited

13. SUPPLEMENTARY NOTES
NUWC2015 The contents of this memo represent the written version of a presentation at the Ocean Seismic-Acoustic Conference held at LaSpezia, Italy June 10-14 1985.

14. ABSTRACT
Long-range sound propagation in the Arctic Ocean is characterized by a refractive surface sound channel with a rough water-ice interface. Recent experimental measurements show that, for frequencies below 100 Hz, attenuation exceeds sea water absorption by two orders of magnitude. The most likely mechanism is scattering from the rough ice canopy. Theoretical estimates of the scattering loss, obtained using the method of small perturbation and statistical measures of the under ice roughness obtained from experimental data, were examined for models of the ice canopy having varying degrees of realism. All theoretical estimates for scattering loss, irrespective of the particular model for the ice canopy, were substantially lower than the measured values of scattering loss. The physics of the loss mechanism is evidently not well understood and evidently additional experimental and theoretical investigations are required.

15. SUBJECT TERMS
Project Reward Jumbo; long-range sound propagation; Arctic Ocean

16. SECURITY CLASSIFICATION OF:			17. LIMITATION OF ABSTRACT	18. NUMBER OF PAGES	19a. NAME OF RESPONSIBLE PERSON
a. REPORT	b. ABSTRACT	c. THIS PAGE			
unclassified	**unclassified**	**unclassified**	**Same as Report (SAR)**	**22**	

PREFACE

The contents of this memo represent the written version of a presentation at the Ocean Seismic-Acoustic Conference held at LaSpezia, Italy June 10-14 1985.

ABSTRACT

Long-range sound propagation in the Arctic Ocean is characterized by a refractive surface sound channel with a rough water-ice interface. Recent experimental measurements show that, for frequencies below 100 Hz, attenuation exceeds sea water absorption by two orders of magnitude. The most likely mechanism is scattering from the rough ice canopy. Theoretical estimates of the scattering loss, obtained using the method of small perturbation and statistical measures of the under ice roughness obtained from experimental data, were examined for models of the ice canopy having varying degrees of realism. All theoretical estimates for scattering loss, irrespective of the particular model for the ice canopy, were substantially lower than the measured values of scattering loss. The physics of the loss mechanism is evidently not well understood and evidently additional experimental and theoretical investigations are required.

ADMINISTRATIVE INFORMATION

This memo was prepared under Project No. C64666 "Project Reward Jumbo, Task 14A". Principal Investigator Dr. F. R. DiNapoli (Code 01Y). The sponsor activity is the Office of Naval Research, Program Manager, J. Brothers (Code 512).

LOW FREQUENCY ATTENUATION IN THE ARCTIC OCEAN

The deep water abyssal plain regions of the Arctic ocean provide almost text book examples of Acoustic Propagation in a range independent ocean at low frequencies if one could ignore the influence of the rough canopy. This can be seen by examining the empirically derived expression and plots of propagation loss versus range shown in Fig. 1.

Shown at the top is an expression for propagation loss empirically derived from data in an abyssal plain of the Arctic ocean. The first two terms ($A + 10\log(R)$) represent the expected result for a range independent ocean. The last term ($\propto R$) is similar in form to the term representing attenuation loss found for ice free waters. We note that for the Arctic, however, this term is predominantly determined by scattering loss from the rough ice canopy, and that it is two orders of magnitude larger than attenuation loss in ice free waters.

The scattering loss was found to have an $f^{3/2}$ dependency which results in a rather significant increase in propagation loss at low frequencies and long ranges as can be seen from an examination of the curves.

This paper summarizes our progress in an ongoing effort to gain insight into this scattering problem.

Measurements of the acoustic field and the underside ice profile were obtained concurrently. A typical section of the ice profile is depicted in the upper left hand corner of Fig. 2. We have tipped the ice upside down so that the air-ice interface is represented by the x-axis. This surface is also rough but appears as a smooth line owing to the lack of concurrent topside roughness measurements. The wavy line above the x-axis is the water-ice interface. We call your attention to the fact that this is a highly compressed view since the horizontal scale is in km and the vertical scale is in m. Although the deepest ice keel shown here is only about 10m, ice keels on the order of 30m are not uncommon.

From the distribution of ice keels shown in the upper right hand corner we find that the mean draft is 4m and the standard deviation of ice keels taken about the mean is 2m.

The normalized auto correlation function is provided in the lower right hand corner. Using the definition that the correlation length, l, is that value of for which the correlation function has the value of .6 (or as it turns out for which it decays to one over e) we find that l equals 44m.

The resulting one dimensional power spectral density is shown in the lower left hand corner along with a smooth curve obtained from an analytic function to be described shortly. The spectrum is found to have F to the minus three frequency dependence.

The values for the parameters shown, namely a mean draft of 4m, =2m and a correlation length of 44m are the average values for these parameters resulting from concurrent measurements of the ice profile and acoustic field obtained over a large portion of the abyssal plain where the experiment was conducted.

The availability of concurrent measurements, which is a rather rare occurence in acoustic scattering, has caused us a fair amount of frustration in our attempt to understand the scattering process. This frustration stems from our inability to obtain the correct answer when using the average values obtained from the concurrent measurements and a theory which we believe is appropriate. On the other hand, if the concurrent measurements are ignored, which is equivalent to using improper values for free ice statistical parameters, and the same theoretical development is employed, it is exceedingly easy to obtain an answer which appears to be correct. The remainder of the paper provides an elaboration of these comments. Our progress to date can thus be summarized as follows: we have not found a satisfactory solution, but we can indicate what the answer cannot be.

Candidate mathematical models of the ice canopy are arranged from top to bottom in decreasing order of realism in Fig. 3. Model I being a full elastic layer is perhaps the most realistic description but it also has the greatest number of free parameters. Only the density, ρ_1, the compressional sound speed, (C_{1p}, the standard deviation of the bottom roughness, $_B$, and the

correlation length of the bottom roughness, l_B , can be considered approximately known.

Model II ignores the elastic properties of ice but still has three free parameters namely, σ_T, l_T , and α_1 which represents absorption loss within the ice.

Finally Model III essentially ignores everything about the ice except for its roughness but has the attractive feature that no free parameters exist if the scattering surface is taken as the bottom of the ice and measured values are used for σ_B and l_B. We thus start with Model III and work our way up in sophistication.

The application of the method of small perturbations (MSP) to underwater acoustic scattering problems has received considerable attention (1-10) in the past and since we believe it is applicable to this problem it is utilized.

The general procedure outlined in Fig. 4 is to utilize the method of small perturbations (MSP) to obtain an expression for the coherent scattered plane wave reflection coefficient which is denoted by $\tilde{R}$.

We make the following observation regarding perturbation theory. First we believe it is applicable at the frequencies of interest and second that experimental results support neglecting the incoherent component of the scattered field for this problem.

We next replace the unperturbed reflection coefficient denoted by $\tilde{R}$, which appears in the Fast Field Program with $\tilde{R}$, insert a measured Arctic sound speed profile and compare FFP predictions to the empirical curves shown previously.

In utilizing MSP we make the assumptions that the statistics of the rough scattering surface are stationary and isotropic. Our measurements of the ice statistics along a line indicate that the statistics are not stationary and if the topside and bottomside roughness characteristics are even loosely correlated then observations of the two dimensional topside rough surface would also indicate that the isotropic assumption is also incorrect. To date we have not quantified the impact of these two incorrect assumptions upon the results to be shown shortly.

The perturbation result for Model III (no layer,

roughness at the pressure release boundary), is well known and given by the double integral on the first line of Fig. 5. Theta sub zero is the incident angle, small k perpendicular and capital k perpendicular are the horizontal wave number components of the incident plane wave and the rough surface respectively. $\tilde{P}_2$ is the two dimensional spectrum of the rough surface which can be related to the measured one dimensional spectrum $\tilde{P}_1$ if we assume isotropic roughness.

We fit the measured data for $\tilde{P}_1$ with the analytical expression given in the middle of the third line up from the bottom and find that it depends on sigma, the correlation length and goes like F to minus three for large values of spatial frequency. Using the analytical fit instead of the actual data proves advantageous for we can then find an analytic expression for the one dimensional, auto correlation function, $N_1(\rho)$ which is given in terms of the correlation length and a modified Bessel function of the first kind.

We also can find the two dimensional isotropic spectrum, which has a form similar to the one dimensional spectrum except that it behaves asymptotically like F to the minus four.

Finally, after some intricate but straightforward manipulations, the scattered reflection coefficient is given by the integral on the bottom line. This integral is evaluated numerically for various frequencies and angles of incidence.

Two approximations (Fig.6) to the scattering integral of Fig. 5 have been frequently used in the past. For the Kirchhoff approximation $\tilde{P}_2$ is replaced by a delta function which yields an auto correlation function approximately equal to unity and thus ignores any contributions from the slopes of the rough surface. The reflection coefficient is then found to have a squared dependency with both frequency and the cosine of the incident angle.

The Marsh approximation which would appear to be valid for shallow grazing angles, is given by an abbreviate version of the scattering integral. Utilizing the analytical fit to the one dimensional spectrum and then carrying out the integration one finds that the reflection coefficient under the Marsh approximation has a three halves dependency on frequency a linear dependency on the cosine of the incident angle

and a dependency on the correlation length.

The reflection loss for all three results namely the exact MSP integral shown as the solid line, the Kirchhoff approximation given by the line with long and short dashes and the Marsh approximation given by the dashed line is provided in Fig. 6 for 47 Hz and σ = 2 and l = 44m. For incident angles between 77 and 90 degrees, which is the region of interest to low frequency Arctic acoustics, the Marsh approximation yields a greater loss and the Kirchhoff approximation less loss than the exact answer. The juxtaposition of the three results in this region remains the same for all frequencies below 100 Hz.

Since the Marsh approximation yields the greatest reflection loss an indication of how well the propagation loss predictions from all three results would compare with the empirical result can be obtained by merely examining the result using the Marsh approximation.

The FFP prediction of propagation loss at 47 Hz using the Marsh approximation and α = 2m and correlation length equal to 44m which were the average values of the ice statistical parameters is given by the wavy line at the top of Fig.7. The empirical fit to the data is provided by the solid line. It is clear that the Marsh approximation provides too little loss at this frequency when the average values for the ice statistical parameters are used. This discrepancy persists for all frequencies spanned by the data.

If concurrent measurements were not available and values for free ice statistical parameters could be assigned arbitrarily perfect agreement with the data can be easily attained at all frequencies with the Marsh approximation merely by changing σ to 3m which is not an unreasonable value.* The result at 47 Hz (displaced by 20 dB) is shown on the lower portion of Fig. 7. One could also obtain excellent agreement with the Kirchhoff approximation at all frequencies if σ is increased to 5m. Thus obtaining agreement with experimental data in the absence of concurrent measurements or equivalently by using free parameters is felt to be a poor criteria for judging the validity of scattering formulas.

If the scattering surface of Model III were taken as the ice-air interface instead of the water-ice interface we suspect the comparison using the average

* The measured values of σ varied between 1 and 3m.

values for σ and 1 would be worse since σ for the topside roughness is a smaller owing to melting and the effects of wind erosion. We thus conclude that Model III is inappropriate.

The perturbation answer for Model II (liquid layer with no roughness at the top and no absorption loss within the layer) is given in terms of the unperturbed reflection coefficient R_2^2 and the double integrals I sub one and I sub two provided in Fig. 8. The M title functions are involved expressions for the acoustic fields in each region evaluated at the mean surface and are provided in Fig. 9.

We make two observations which hopefully provide some insight into the results for Model II. First the unperturbed reflection coefficient has unit magnitude for all incident angles. This results because the absorption in the layer has been set to zero and the pressure release surface behind the layer perfectly reflects any transmitted energy back into the water. Thus the presence of a critical angle has no special significance to the problem. The second point to note is that the difference in densities between the two media is almost zero.

The reflection loss for Model II, under the Kirchhoff approximation and with σ= 2 and l = 44m is given by the dotted line in Fig. 10. Recalling that the unperturbed reflection coefficient has unit magnitude, the influence of the roughness at the bottom of the layer is determined by the deviation of the curve from zero. The Kirchhoff result for Model III (roughness at pressure release surface) discussed previously is overplotted as the solid line. Since the solid line result provided too little loss, utilizing the average statistics, (see upper portion of Fig. 7) then it is clear that the liquid layer will fall short by a wide margin. As frequency increases the deviation of Model II from zero does increase slightly but in all cases is considerably less than the Kirchhoff result for Model III. We believe the factor controlling the scattering for Model II is the difference in density on either side of the scattering surface. Since this difference is almost zero the scattering loss is small and it is unlikely that the answer would change substantially if the full MSP integrals were evaluated instead of making the Kirchhoff approximation.

We thus conclude that Model II although apparently

more realistic than Model III actually provides poorer results and thus is also inappropiate.

This summarizes our progress to date. In the future we shall examine the answers provided by Model I which was the full elastic layer. * Considering the number of free parameters which exist for that problem, however, we do not believe a convincing case can be made until measured values for the elastic properties of sea ice become available. We also plan to examine the influence of a rough surface which is not isotropic and where statistics are non-stationary.

* Subsequent to this presentation W. Kuperman of NRL and H. Schmidt of SACLANT RNN Model I using realistic values for shear speed, absorption within the ice, and the measured roughness parameterms of σ =2m and ℓ =4m. The scattering loss using the full elastic layer was found to be comparable to that obtained from Model II and substantially less than that from Model III which was substantially less than the measured scattering loss.

REFERENCES

1. H. Wysor Marsh, M. Schulkin, and S.G. Kneale, Scattering of Underwater Sound by the Sea Surface, J. Acoust. Soc. Am., Vol. 33, Number 3, (March 1961).

2. E. Y. T. Kuo, Wave Scattering and Transmission at Irregular Surfaces, J. Acoust. Soc. Am., Vol. 3, Number 11, (Nov., 1964).

3. F. G. Bass, I. M. Fuks, "Wave Scattering from Statistically Rough Surfaces", Pergamon Press, New York, (1979).

4. Yu. P. Lysanov, Part IV, Scattering of Sound by Irregular Surfaces, from "Acoustics of the Ocean", USSR Academy of Sciences, Acoustics Institute, Nauka Press, Moscow, 1974. NISC Translation No. 4048, (Oct., 1978).

5. J. A. DeSanto, Chapt. II, "Ocean Acoustics", Springer-Verlag, New York, (1979).

6. William A. Kuperman, Coherent Component of Specular Reflection and Transmission at a Randomly Rough Two-fluid Interface, J. Acoust. Soc. Am., Vol. 58, No. 2, (Aug., 1975).

7. L. M. Brekhovskikh, Yu, P. Lysanov, Chapt. IX, "Fundamentals of Ocean Acoustics", Springer-Verlag, New York, (1982).

8. A. D. Lapin, Scattering of Sound by a Solid Layer with Rough Boundaries, translated from Akusticheskii Zhurnal, Vol. 12, No. 1., (Jan.-Mar., 1966).

9. F. I. Kryazhev, V. M. Kudryashov, and N. A. Perov, Propagation of Low-frequency Sound Waves in a Waveguide with Irregular Boundaries, Sov. Phys. Acoust., Vol. 22, No. 3, (May-Jun., 1979).

10. F. I. Kryazhev, and V. M. Kudryashov, Sound Field in a Waveguide with a Statistically Rough Admittance Boundary", Sov. Phys. Acoust., Vol. 30, No. 5 (Spt.-Oct., 1984).

11. F. R. DiNapoli, R. L. Deavenport, Theoretical and Numerical Green's Function Field Solution in a Plane Multilayered Medium, J. Acoust. Soc. Am., Vol. 67, No. 1, (Jan., 1980).

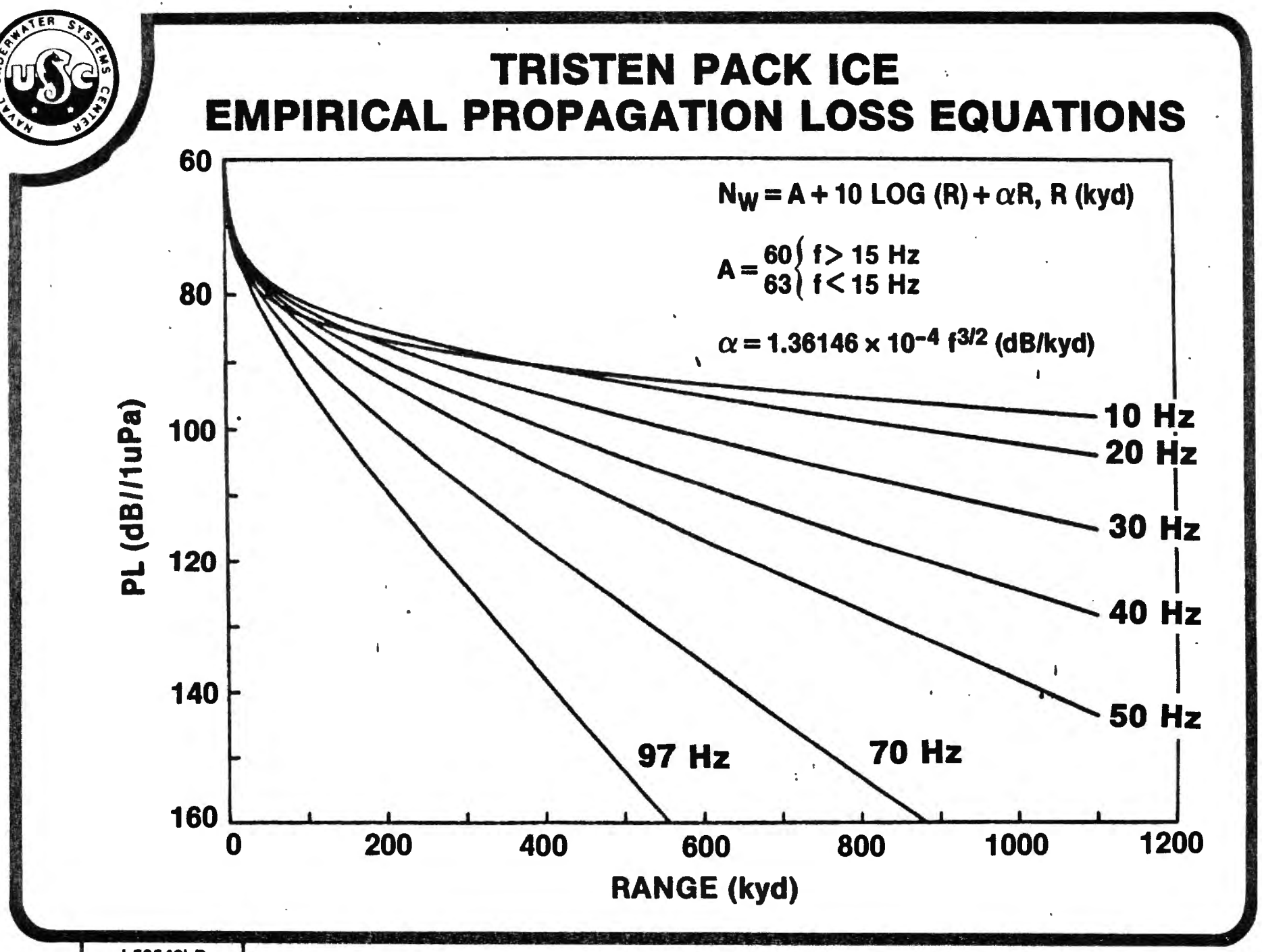

L50542bP

Figure 1

TM 851130

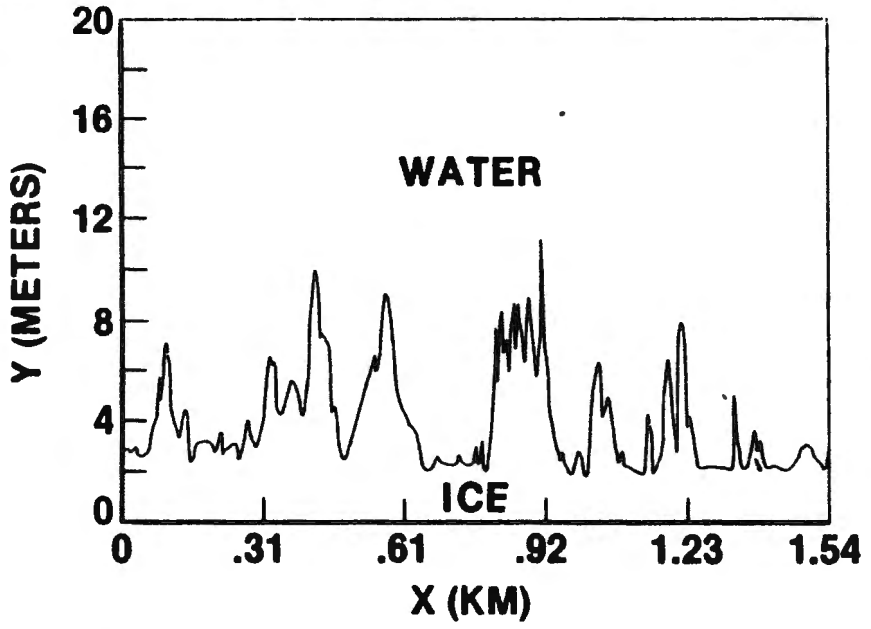

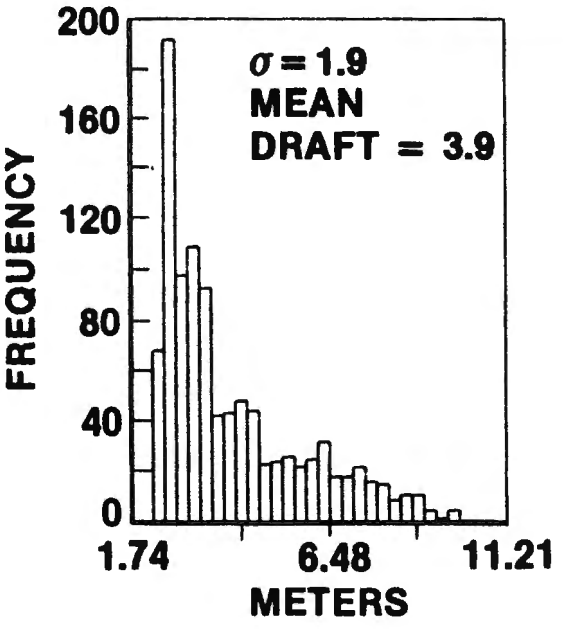

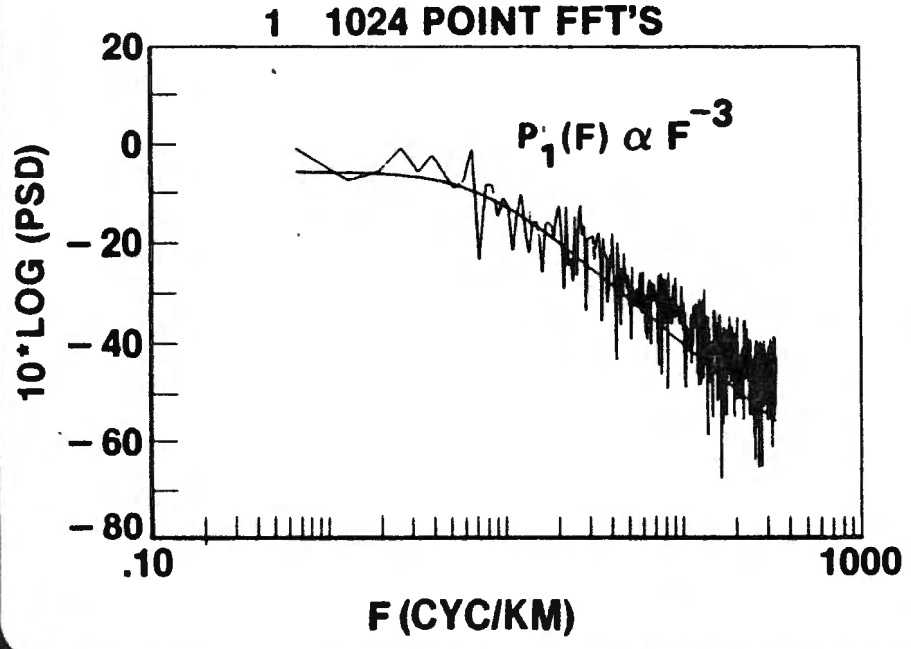

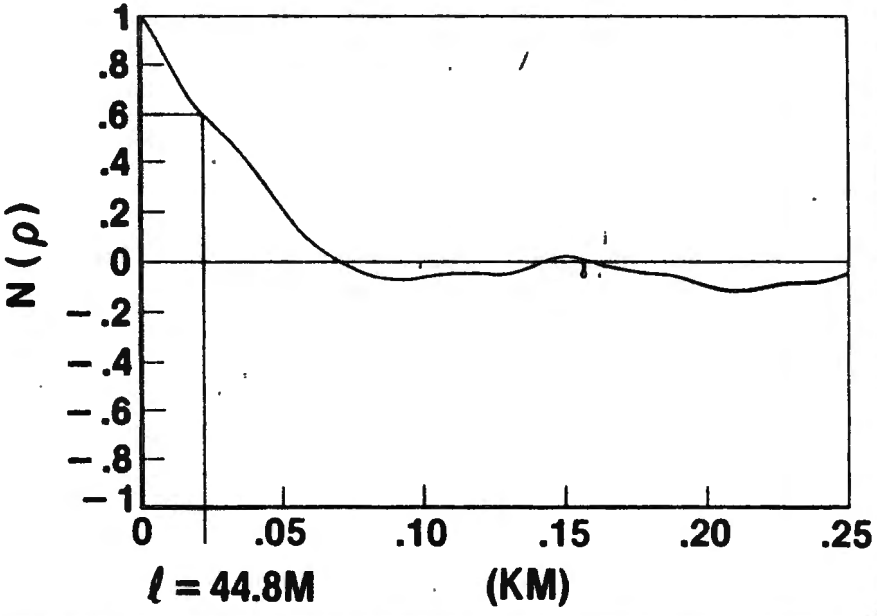

L50542cP

Figure 2

TM 851130

MATHEMATICAL MODELS FOR SCATTERED PLANE WAVE REFLECTION COEFFICIENT

MODEL I (FULL ELASTIC LAYER)

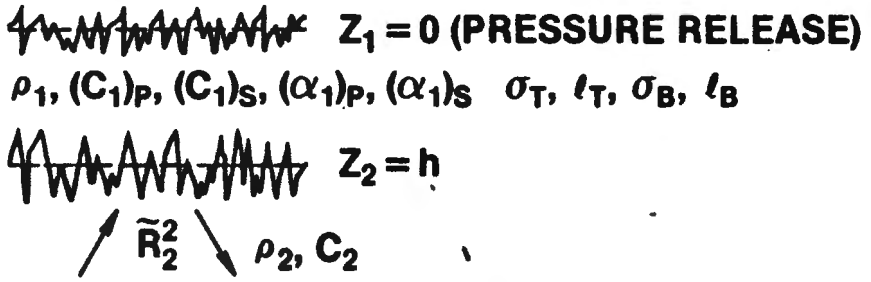

MODEL II (LIQUID LAYER)

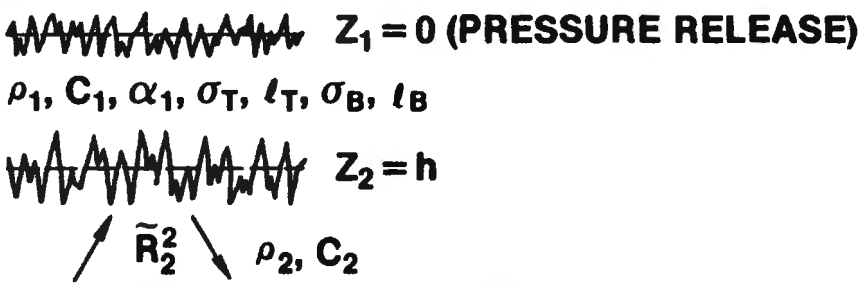

MODEL III (NO LAYER, ROUGHESS AT PRESSURE RELEASE SURFACE)

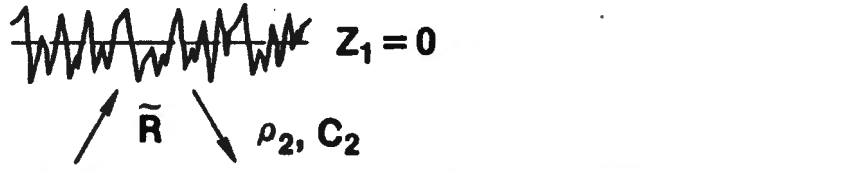

- START WITH MODEL III, WORK UP TO MODEL I

L50542gP

Figure 3

TM 851130

MODEL III (NO LAYER, ROUGHNESS AT PRESSURE RELEASE SURFACE)

FULL PERTURBATION THEORY

$$\tilde{R}(f,\theta_0,\sigma,\ell) = -1+k\cos\theta_0\,\frac{\sigma^2}{\pi}\int d\vec{k}_\perp \tilde{P}_2(\vec{K}_\perp)\left\{k_2^2-(\vec{k}_\perp-\vec{K}_\perp)\cdot(\vec{k}_\perp-\vec{K}_\perp)\right\}^{1/2}$$

$\vec{k}_\perp$; HORIZONTAL WAVENUMBER COMPONENT OF INCIDENT PLANE WAVE

$\vec{K}_\perp$; HORIZONTAL WAVENUMBER COMPONENT OF ROUGH SURFACE

— ASSUMING ISOTROPIC ROUGHNESS

$\tilde{P}_2 = \tilde{P}_{21}$ WHICH IS RELATED TO MEASURED $\tilde{P}_1$

— USING ANALYTIC FIT TO $\tilde{P}_1(F)$, F SPATIAL FREQUENCY FIND

$$N_1(\rho) = (2/\ell)\,K_1[(2/\ell)\rho] \quad \tilde{P}_1(F) = \frac{\pi(2\sigma/\ell)^2}{[(2/\ell)^2+(2\pi F)^2]}\,3/2 \quad \simeq F^{-3} \text{ FOR LARGE F}$$

AND

$$\tilde{P}_{21}(F) = \frac{4\pi(2\sigma/\ell)^2}{[(2/\ell)^2+(2\pi F)^2]}\,2 \quad \simeq F^{-4} \text{ FOR LARGE F}$$

$$\tilde{R} = -1+k^4\cos\theta_0\,(\sigma\ell)^2\int_0^{\pi/2}\frac{d\theta\,\cos^2\theta\,\sin\theta\left\{1+\left(\frac{k\ell}{2}\right)^2(\sin^2\theta+\sin^2\theta_0)\right\}}{\left\{\left[1+\left(\frac{k\ell}{2}\right)^2(\sin^2\theta+\sin^2\theta_0)\right]^2-\left[\left(\frac{k\ell}{2}\right)^2\sin\theta\,\sin\theta_0\right]^2\right\}}\,3/2$$

L50542fP

Figure 4

TM 851130

MODEL III (NO LAYER, ROUGHNESS AT PRESSURE RELEASE SURFACE)

KIRCHHOFF APPROXIMATION

$k\ell \gg 1,\ k\ell \cos^2\theta_0 \gg 1$ (APPROPRIATE FOR STEEP GRAZING ANGLES)

$$\tilde{P}_2(\vec{K_\perp}) \cong 2\pi\,\delta^2(\vec{K_\perp}) \qquad N_2(\rho) \cong 1 \qquad \frac{dN_2}{d\rho}(\rho) \cong 0$$

$$\tilde{R}(f, \theta_0, \sigma) \cong -1 + 2\sigma^2 k^2 \cos^2\theta_0$$

MARSH APPROXIMATION

$k\ell \gg 1,\ k\ell \cos^2\theta_0 \ll 1$ (APPROPRIATE FOR SHALLOW GRAZING ANGLES)

$$\tilde{R} \cong -1 + 2\sqrt{2}\, k^{3/2} \cos\theta_0\, \sigma^2 \int d|K_\perp| \tilde{P}_2(|K_\perp|)\, |K_\perp|^{3/2}$$

USING MEASURED $\tilde{P}_1$ FIND

$$\tilde{R}(f, \theta_0, \sigma, \ell) \cong -1 + 2.396 \frac{k^{3/2}}{\ell^{1/2}} \cos\theta_0\, \sigma^2\, e^{i\pi/4}$$

L50542hP

Figure 5

TM 851130

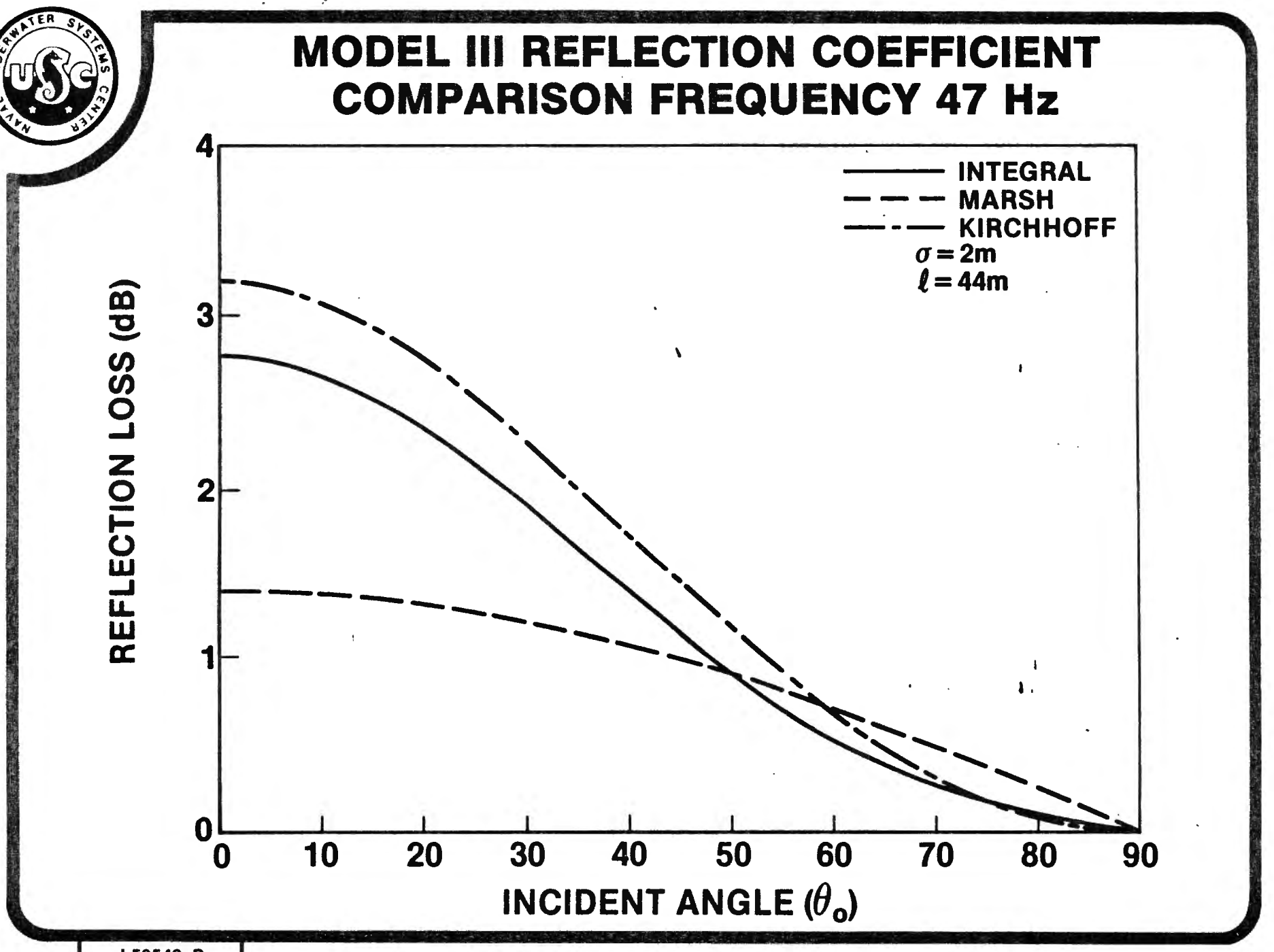

L50542aP

Figure 6

COMPARISON OF MARSH APPROXIMATION WITH EXPERIMENTAL DATA

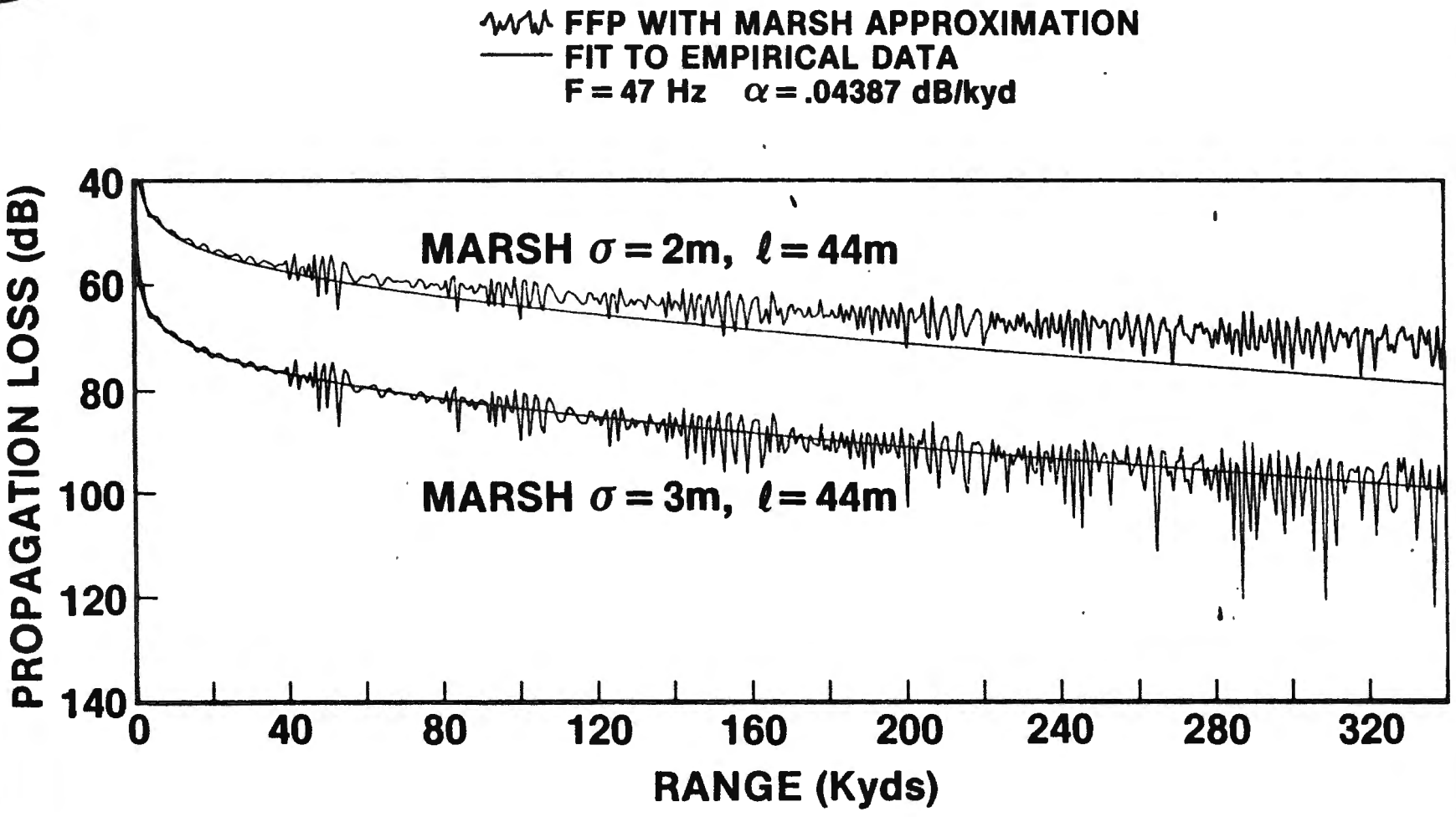

L50542dP

Figure 7

MODEL II (LIQUID LAYER, WITH NO ATTENUATION, NO ROUGHNESS AT TOP)

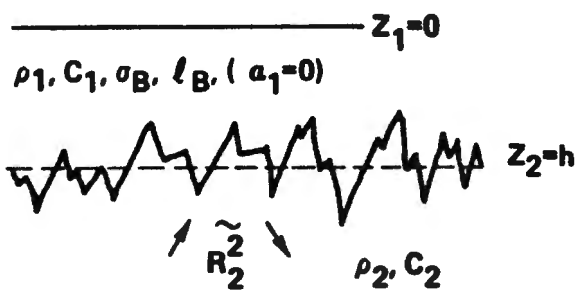

$$\tilde{R}_2^2 = R_2^2 + \frac{\sigma^2}{2\rho_2 k_{2z}} \left\{ -k_{2z}(1-R_2^2) I_1 + \rho_2 (1+R_2^2) I_2 \right\}$$

$$I_1 = \frac{1}{2\pi} \int d\xi_\perp^* \, \Delta_c^{-1}(\xi_{1z}, \xi_{2z}) \, \tilde{P}_2(k_\perp^* - \xi_\perp^*) \, \tilde{M}(\xi_\perp^*, k_\perp^*)$$

$$I_2 = \frac{1}{2\pi} \int d\xi_\perp^* \, \Delta_c^{-1}(\xi_{1z}, \xi_{2z}) \, \tilde{P}_2(k_\perp^* - \xi_\perp^*) \left\{ \tilde{M}_2(k_\perp^* \xi_\perp^*) - \tilde{M}_3(\xi_\perp^*, k_\perp^*) \, \xi_\perp^* \cdot (\xi_\perp^* - k_\perp^*) \right\}$$

R_2^2 – UNPERTURBED PLANE WAVE REFLECTION COEFFICIENT

$c_1 > c_2$ RESULTING IN CRITICAL ANGLE

$|R_2^2| \equiv 1$ FOR ALL ANGLES

$\rho_1 \cong \rho_2$

L50542eP

Figure 8

TM 851130

MODEL II (LIQUID LAYER, WITH NO ATTENUATION, NO ROUGHNESS AT TOP)

$$\tilde{m}_1(\vec{\xi}_\perp, \vec{k}_\perp) = -i(\rho_1-\rho_2)^2 \frac{d\phi_1}{dz} k_{2z}(1-R_2^2)\xi_{2z} - \rho_2(\xi_{2z}\phi_1 + i\frac{d\phi_1}{dz})(1+R_2^2)(\rho_2 k_{1z}^2 - \rho_1 k_{2z}^2)$$

$$-\rho_2(\xi_{2z}\phi_1 + i\frac{d\phi_1}{dz})(1+R_2^2)(\rho_1-\rho_2)\vec{k}_\perp \cdot (\vec{\xi}_\perp - \vec{k}_\perp)$$

$$\tilde{m}_2(\vec{\xi}_\perp, \vec{k}_\perp) = -[i\xi_{2z}^2 \frac{d\phi_1}{dz} - \xi_{2z}\frac{d^2\phi_1}{dz^2}] k_{2z}(\rho_1-\rho_2)(1-R_2^2)$$

$$+\frac{(1+R_2^2)}{\rho_1}[\rho_1\xi_{2z}^2\phi_1 + \rho_2\frac{d^2\phi_1}{dz^2}][(\rho_2 k_{1z}^2 - \rho_1 k_{2z}^2) + (\rho_1-\rho_2)\vec{k}_\perp \cdot (\vec{\xi}_\perp - \vec{k}_\perp)]$$

$$\tilde{m}_3(\vec{\xi}_\perp, \vec{k}_\perp) = -[-i\frac{d\phi_1}{dz} - \xi_{2z}] k_{2z}(\rho_1-\rho_2)(1-R_2^2)$$

$$-[\rho_1\phi_1 - \rho_2](\frac{1+R_2^2}{\rho_1})[(\rho_2 k_{1z}^2 - \rho_1 k_{2z}^2) + (\rho_1-\rho_2)\vec{k}_\perp \cdot (\vec{\xi}_\perp - \vec{k}_\perp)]$$

$\phi_1(\xi_{1z}, z)$ — DEPTH DEPENDENT PORTION OF FIELD IN LAYER

L50544yP

Figure 9

TM 851130

MODEL II REFLECTION COEFFICIENT FREQUENCY 47 Hz

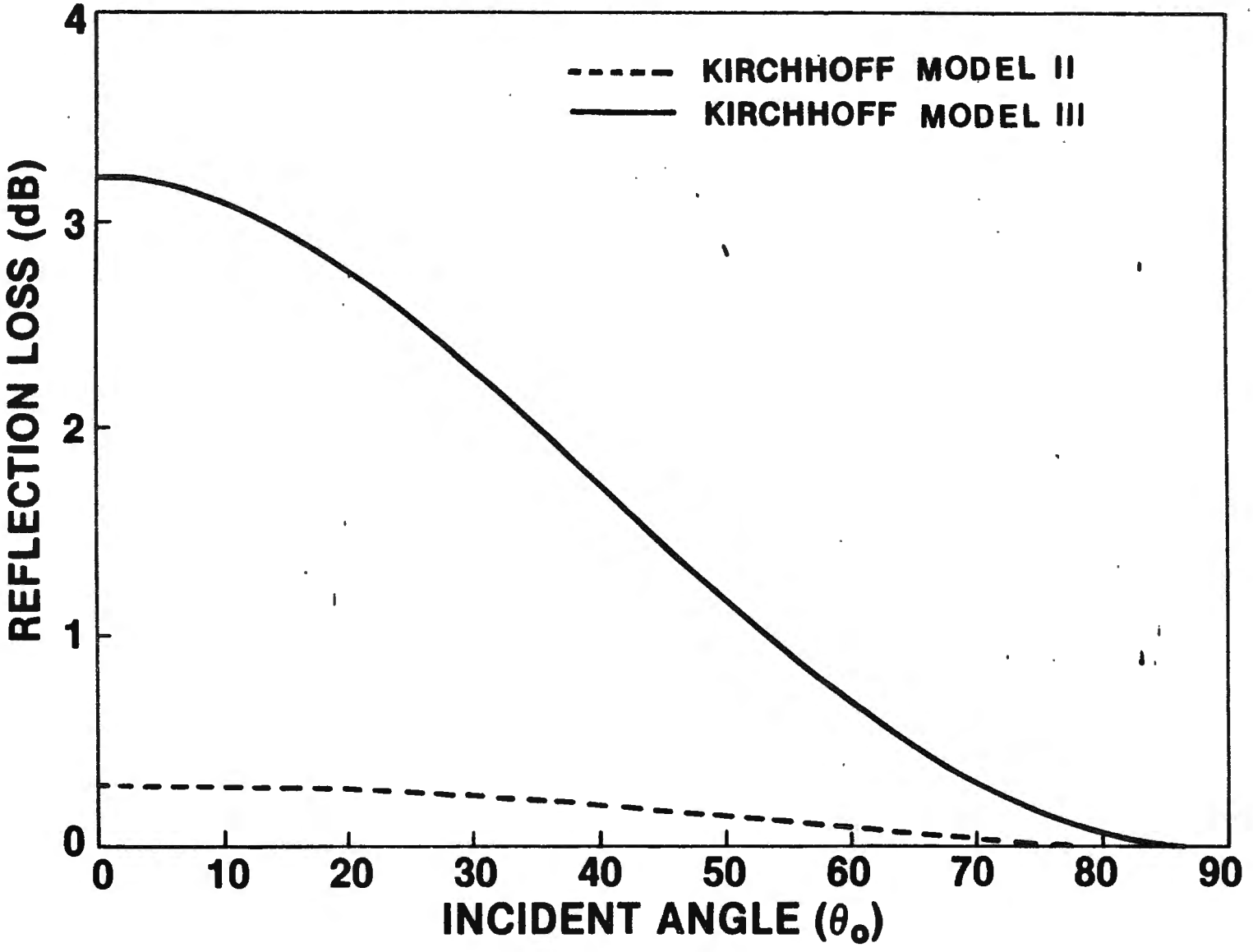

Figure 10

EXTERNAL DISTRIBUTION LIST

COMSUB DEVRON 12 (CDR. O. B. Cooke, D. McKinley)

NORDA (R. Gardner, G. Gotthardt, R. Martin, D. Ramsdale)

CNO, OP 223 (Lcdr. R. C. Barnes)

OP, 951-F (Capt. M. Schneider) (3)

Polar Research Laboratory (J. Wilson, B. Buck)
N00123-80-C-0042

ASL, NOSC Code 19 (Capt. J. Sabol, Dr. G. Dreyer,
Capt. M. Dorman)

COMSUBPAC (Code 24, LCDR. R. Pohtos)

ORI, Inc. (V. Simmons)
N0014-82-C-0820

MIT, Dept. of OE Rm 5-317 (Profs. I. Dyer, A. Baggeroer,
P. N. Mikhalevsky, G. Duckworth,
Lt. J. Polcari)

SAI (R. Greene) N00014-85-C-0084

Signatron (J. Pierce) N00120-82-G-B286-0003

LDGO (H. Kutschale)

NRL (O. Diachok, W. Kuperman, R. Dicus, A. Tolstoy)

SACLANT (F. Jensen, H. Schmidt, J. Akal)

Catholic U. (J. J. McCoy, L. Fishman)

NDRE (I. Engelsen, J. Glattertre, E. Hug)

SCRIPPS (W. Munk, F. Fisher)
N00024-82-C-6400

DREP. (D. Thomson, G. Brooke)

ARL/Penn State (D. F. McCammon)

APL/U. of Washington (R. Francoise)

NOSC (H. Bucker,D. Gordon)

WHOI (J. Flynch, G. Frisk, R. Spindel)

Viriginia Technical University (Prof. W. Kohler)

INTERNAL DISTRIBUTION LIST

Code 01Y, (R. Russell, Lt. P. Hill, LCDR. R. Eyman, J. Donald, M. Ahrens, F. DiNapoli (4))

Code 10

Code 32, (J. Martins, C. Peroskie, G. Austin, G. Kudlak, D. Hicks, L. Cormier)

Code 33, (W. Roderick, P. Koenings, R. Nielsen, D. Potter, M. Fecher, R. Deavenport, D. Browning, E. Kuo, D. Lee, G. Botseas, A. Nuttall)

Code 38, (G. Santos)

Code 36, (M. Buffman)

Code 35, (C. Gardner, S. McCarthy, J. Short)

Code 60